Prodrugs of Perzinfotel with Improved Oral Bioavailability

Reinhardt B. Baudy,[†] John A. Butera,[†] Magid A. Abou-Gharbia,[†,‡] Hong Chen,[†] Boyd Harrison,[†] Uday Jain,[†] Ronald Magolda,[†] Jean Y. Sze,[†] Michael R. Brandt,[§,||] Terri A. Cummons,[§] Diane Kowal,[§] Menelas N. Pangalos,[§] Bojana Zupan,[§,⊥] Matthew Hoffmann,[#] Michael May,[#] Cheryl Mugford,[#] Jeffrey Kennedy,[§] and Wayne E. Childers, Jr.*[,†]

Chemical & Screening Sciences, Wyeth Research, CN-8000, Princeton, New Jersey 08543, Neuroscience Discovery Research, Wyeth Research, Princeton, New Jersey, and Wyeth Drug Safety & Metabolism, Collegeville, Pennsylvania

Received September 26, 2008

Previous studies with perzinfotel (**1**), a potent, selective, competitive NMDA receptor antagonist, showed it to be efficacious in inflammatory and neuropathic pain models. To increase the low oral bioavailability of **1** (3−5%), prodrug derivatives (**3a**−**h**) were synthesized and evaluated. The oxymethylene-spaced diphenyl analogue **3a** demonstrated good stability at acidic and neutral pH, as well as in simulated gastric fluid. In rat plasma, **3a** was rapidly converted to **1** via **2a**. Pharmacokinetic studies indicated that the amount of systemic exposure of **1** produced by a 10 mg/kg oral dose of **3a** was 2.5-fold greater than that produced by a 30 mg/kg oral dose of **1**. Consistent with these results, **3a** was significantly more potent and had a longer duration of activity than **1** following oral administration in a rodent model of inflammatory pain. Taken together, these results demonstrate that an oxymethylene-spaced prodrug approach increased the bioavailability of **1**.

Introduction

Excitatory amino acids (EAAs[a]) acting at the *N*-methyl-D-aspartate-selective (NMDA) subtype of the glutamate receptor play a role in both acute and chronic pain. Increases in afferent input and glutamate release within the spinal cord have been observed after peripheral injection of irritants (e.g., carrageenan) or tissue injury.[1−3] In preclinical studies, NMDA antagonists reverse neuronal hyperexcitability as well as hyperalgesia in several inflammatory and neuropathic pain models associated with various pathophysiologic mechanisms.[4−6] However, among clinically assessed NMDA antagonists, the narrow separation between effectiveness and liabilities, such as sedation and psychotomimetic effects, has severely hampered their utility for the treatment of neuropathic pain.[7]

We previously described perzinfotel (**1**, EAA-090, [2-(8,9-dioxo-2,6-diazabicyclo[5.2.0]non-1(7)-en-2-yl)ethyl]phosphonic acid) as a potent, competitive NMDA receptor antagonist. It is selective for the NMDA receptor, showing no significant affinity at over 60 other receptor, enzyme, and ion channel binding sites.[8−10] Previous studies demonstrated **1** to be efficacious in a variety of pain models.[11] However, **1** demonstrates low bioavailability following oral administration.[11] In the current study, we prepared and evaluated oxymethylene-spaced prodrugs of **1** to determine whether they would show improved oral bioavailability. We required a prodrug that would be stable in a wide pH range and physiological fluids and yet decompose rapidly once it reached the plasma. We focused on steric hindrance around the initial site of hydrolysis as a means of controlling the rate of decomposition of our prodrug candidates.

Chemistry

A series of bis-phosphonate derivatives of **1** (compounds **3a**−**h**, Scheme 1) was prepared in a straightforward manner starting from **1** as depicted in Scheme 1. Treatment of **1** with the appropriate chloromethyl ester in the presence of *N*,*N*-diisopropylethylamine in dimethylformamide at 70 °C for 20 h provided the desired prodrug candidates **3a**−**g** in moderate to excellent yield. In order to investigate an oxymethylene spaced carbonate analogue as a potential prodrug moiety, we prepared compound **3h** in the same manner as **3a**−**g** using chloromethyl isopropyl carbonate (**9**).

Noncommercially available chloromethyl ester reagents **4**−**8** were prepared as shown in Scheme 2 by treatment of the appropriate acid chloride with a suitable aldehyde in the presence of zinc chloride. The isopropyl carbonate starting material **9** was synthesized by treating chloromethyl chloroformate with isopropanol. The branched oxymethylene prodrug candidates **3d**−**f** (where $R_1 = CH_3$) were obtained as diastereomeric mixtures. In the case of phenyl derivatives **3d** and **3e**, the two diastereomers were separated successfully by HPLC and evaluated separately. In the case of cyclohexyl analogue **3f**, the diastereomeric mixture was evaluated without prior separation. All compounds were fully characterized by ^{1}H NMR, MS, and combustion analysis.

[^{14}C]-Labeled **1** and [^{14}C]-labeled **3a** were provided by Amersham Life Sciences[12] starting from [^{14}C]-diethyl squarate. [^{14}C]-**1** was prepared using synthetic methodology described

* To whom correspondence should be addressed. Phone: 732-274-4253. Fax: 732-274-4505. E-mail: childew@wyeth.com.
† Chemical & Screening Sciences, Wyeth Research.
‡ Current address: Temple University School of Pharmacy, Philadelphia, PA.
§ Neuroscience Discovery Research, Wyeth Research.
|| Current address: Johnson & Johnson Research and Development, L.L.C., Spring House, PA.
⊥ Current address: Weill Cornell Medical School, New York, NY.
Wyeth Drug Safety & Metabolism.

[a] Abbreviations: AMPA, α-amino-3-hydroxy-5-methylisoxazolepropionate; AUC, area under the curve; C_{max}, maximum concentration; EAA, excitatory amino acid; ESI, electrospray ionization; ^{1}H NMR, proton nuclear magnetic resonance spectroscopy; HPLC, high pressure liquid chromatography; LC/MS, liquid chromatography/mass spectrometry; MS, mass spectrometry; NMDA, *N*-methyl-D-aspartate; PGE_2, prostaglandin E2; po, oral administration; SGF, simulated gastric fluid; SIBLM, simulated intestinal bile fluid; SIF, simulated intestinal fluid; $t_{1/2}$, half-life; TCP, *N*-[1-(2-thienyl)cyclohexyl]-3,4-piperidine; T_{max}, time after dosing at which maximum concentration occurs.

10.1021/jm8011799 CCC: $40.75
Published on Web 01/15/2009

Scheme 1. Synthesis of Bis-phosphonate Ester Prodrugs **3a**−**h**[a]

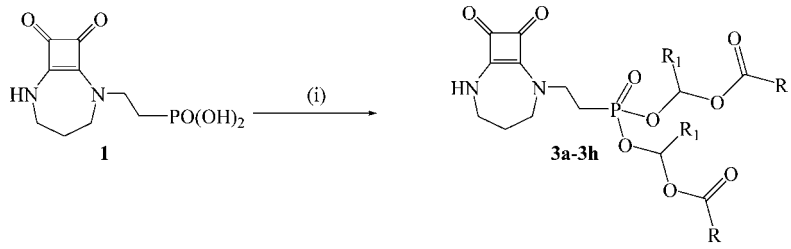

RCOOCHR'Cl*	Product (3)
4	**a**: R = phenyl; R_1 = H
commercially available	**b**: R = t-butyl; R_1 = H
5	**c**: R = cyclohexyl; R_1 = H
7	**d**: R = phenyl; R_1 = methyl (diastereomer 1)
7	**e**: R = phenyl; R_1 = methyl (diastereomer 2)
8	**f**: R = cyclohexyl; R_1 = methyl (mixture)
6	**g**: R = hept-4-yl; R_1 = H
9	**h**: R = isopropyloxy; R_1 = H

[a] Reagents and conditions: (i) *N*,*N*-diisopropylethylamine, dimethylformamide, *RCOOCHR′Cl, 70 °C, 20 h.

Scheme 2. Synthesis of Chloromethyl Ester Intermediates[a]

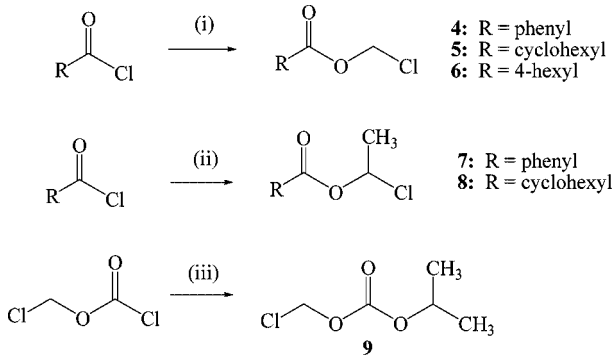

[a] Reagents and conditions: (i) paraformaldehyde, $ZnCl_2$, 0 °C, followed by 55 °C, 20 h; (ii) acetaldehyde, $ZnCl_2$, −20°C, 1 h, followed by room temperature, 20 h; (iii) 2-propanol, pyridine, 0°C, followed by room temperature, 20 h.

previously;[8] [^{14}C]-**3a** was prepared from [^{14}C]-**1** using the methodology described above.

Pharmacology and Pharmacokinetics

Affinities for the competitive NMDA (glutamate), strychnine-sensitive glycine, kainate, and AMPA binding sites were assessed as the compounds' ability to displace the tritiated standard ligands CGP-39653, glycine, kainic acid, and α-amino-3-hydroxy-5-methylisoxazole-4-propionic acid, respectively, as previously described.[10] Functional NMDA antagonism was assessed using a glutamate-stimulated TCP binding assay.[10] Efficacy versus inflammatory pain was measured using a PGE_2-induced thermal hypersensitivity model.[11] In vitro plasma and physiological stability assays were carried out at 37 °C as described below. Pharmacokinetic and radioactive biodistribution studies were performed in male Sprague−Dawley rats. Compounds were administered by oral gavage.

Results and Discussion

With the aim of improving oral bioavailability, a series of oxymethylene-spaced prodrugs of **1** was synthesized and evaluated (**3a**−**h**). We believed that the prodrugs would decompose to **1** via a stepwise mechanism that involved intermediate formation of the hemiesters **2a**−**h** (Figure 1). The structures of the intermediate hemiesters were established during the course of plasma stability studies using (+ESI) and (−ESI) LC/MS. The actual hydrolysis step is believed to occur on the carbon ester, with subsequent elimination of the aldehyde-derived linker to give the phosphonic acid. Therefore, in order to test the effects of electronics and steric hindrance on the hydrolysis, we prepared prodrug candidates with both aromatic and aliphatic ester groups as well as oxymethylene linkers derived from both formaldehyde and acetaldehyde.

Compounds **3a**−**h** were initially evaluated for their stability in rat plasma. From previous studies, it was known that compound **1** possesses an adequate half-life in vivo ($t_{1/2}$ = 1.3−7.8 h, depending on dose).[11] Therefore, we felt that a successful prodrug candidate would undergo rapid, complete conversion to the parent compound **1** in the plasma (within 1−3 h) rather than a slow, continuous release. The results of this initial test are shown in Figure 2. Hydrolysis of the *tert*-butyl (**3b**) and 4-heptyl (**3g**) analogues derived from formaldehyde required 7 h. Analogues derived from acetaldehyde (**3d**−**f**) took even longer, achieving only 30−40% conversion within the 7 h time frame. Compounds **3a**, **3c**, and the carbonate derivative **3h** displayed adequate kinetics and met the initial criteria for advancement.

The three advanced prodrug candidates **3a**, **3c**, and **3h** were evaluated for physiological stability in buffers ranging from pH 1 to pH 9 as well as in SGF, SIF, and SIBLM. Compounds were dissolved in a 9:1 mixture of the appropriate test reagent (buffers, SGF, etc.) and acetonitrile according to the procedure described in the Supporting Information and examined by LC/MS at regular intervals. The structures of the prodrugs, the hemiesters, and **1** were confirmed by their MS spectra. At 4 h, all three compounds demonstrated good stability in solution at pH values ranging from 1 to 7.4 but were unstable at pH 9. All three candidates were stable in simulated gastric fluid; however, compounds **3a** and **3h** were more stable than **3c** when tested in simulated intestinal fluid (Table 1). The low melting point of **3h** (60−79 °C) made compound **3a** (mp = 127−128 °C) the more attractive drug candidate. Compound **3a** was selected for further evaluation.

The results of detailed physiological stability assays at 37 °C for **3a** are summarized in Tables 2 and 3. Compound **3a** was relatively stable in buffers ranging from pH 1 to pH 7.4, as well as SGF and SIBLM. Considerable conversion to **1** was observed in pH 8.5 buffer and in SIF after 4 h. The conversion

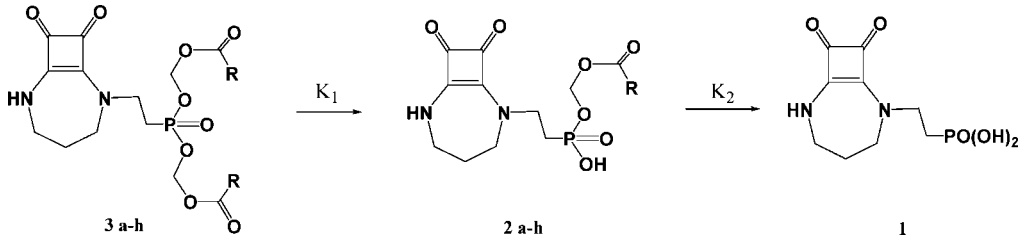

Figure 1. Conversion of bis-phosphonate prodrugs to **1**.

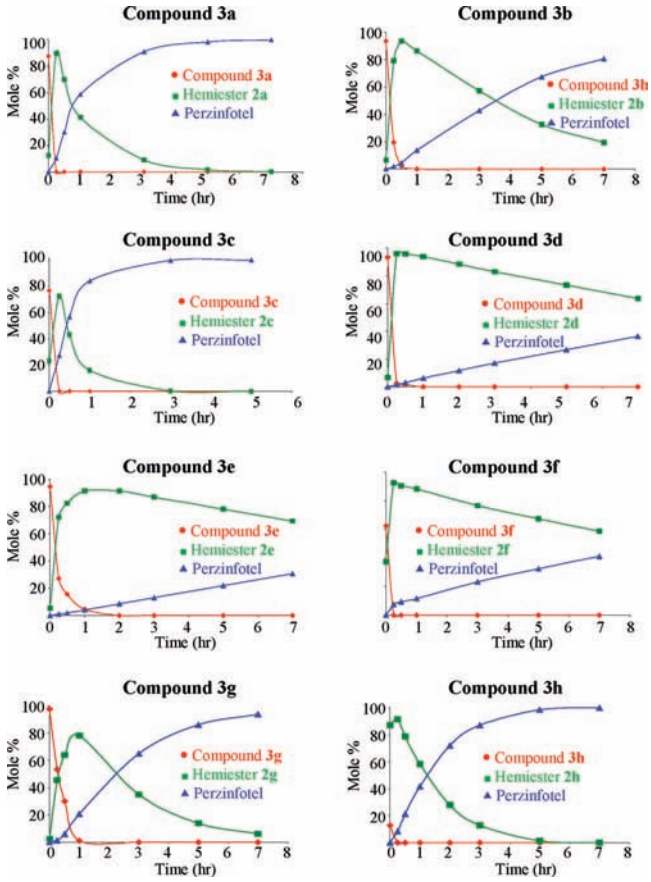

Figure 2. Stability of compounds **3a**−**h** in rat plasma at 37 °C.

Table 1. In Vitro Physiological Stability of **3a**, **3c**, and **3h** (Expressed as Percent Remaining after 4 h)

compd	pH 1.0	pH 4.5	pH 6.6	pH 7.4	pH 9.0	SGF[a]	SIF[b]
3a	99.7	100.2	98.1	91.6	21.2	99.6	43.4
3c	89.0	99.4	95.0	94.4	17.9	91.6	0.0
3h	100.1	100.0	97.7	94.1	7.0	100.0	33.8

[a] Simulated gastric fluid. [b] Simulated intestinal fluid.

products identified included benzoic acid, the hemiester intermediate **2a**, and the parent molecule **1**. After 24 h of incubation, the prodrug **3a** was essentially gone. However, the hemiester **2a** appeared to be significantly more stable, with 75% still remaining after 24 h.

The stability of **3a** in rat plasma was examined in detail at various time points (0, 0.25, 0.5, 1, 3, 5, and 7 h). The conversion of **3a** to the hemiester **2a** was rapid (Figure 3). In less than 15 min the concentration of **3a** was below the level of detection. The conversion of **2a** to **1** was relatively slower, requiring 3 h to generate around 90% of the total expected molar percent of **1**. The identities of **2a** and **1** in this assay were confirmed by LC/MS. Evaluation of the kinetics of conversion of **3a** to **1** in pH 8.5 buffer, SIF, and rat plasma indicates that

Table 2. In Vitro Physiological Stability of **3a** in Various Buffers, Simulated Gastric Fluid (Expressed as Percent Remaining at Indicated Time)

hour	pH 1.0	pH 4.5	pH 6.6	pH 7.4	SGF[a]	SIBLM[b]
0	100.0	100.0	100.0	100.0	100.0	100.0
4	99.7	100.2	98.1	91.6	99.6	99.5
8	99.3	100.0	95.7	83.2	99.3	99.3
12	98.9	99.8	93.7	75.6	99.0	98.6
16	98.5	99.7	91.5	68.7	98.7	98.6
20	98.0	99.5	89.4	62.2	98.3	98.5
24	97.9	99.5	87.4	56.7	98.0	98.1

[a] Simulated gastric fluid. [b] Simulated intestinal bile fluid.

Table 3. In Vitro Physiological Stability of **3a** in pH 9.0 Buffer and Simulated Intestinal Fluid (Expressed as Percent Remaining at Indicated Time)

	pH 9.0			SIF[a]		
hours	**3a**	**2a**	**1**	**3a**	**2a**	**1**
0	99.5	0.5	0.0	99.5	0.5	0.0
4	21.6	74.6	3.8	43.4	55.4	1.2
8	4.7	87.0	8.3	22.1	71.5	6.4
12	1.1	86.4	12.5	12.0	77.6	10.4
16	0.3	82.9	16.9	6.7	78.8	14.6
20	0.1	79.1	20.9	3.7	77.7	18.6
24	0.0	75.3	24.8	2.2	75.4	22.5

[a] Simulated intestinal fluid.

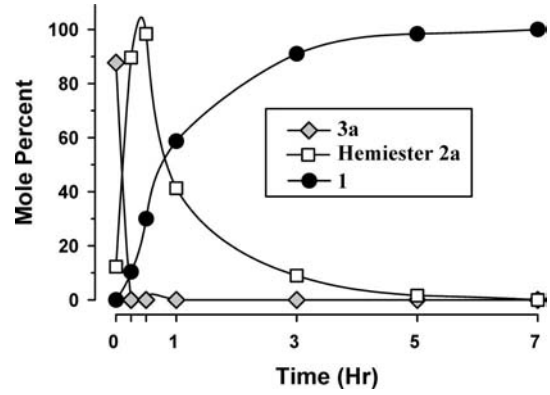

Figure 3. Conversion rate of **3a** in rat plasma at 37 °C: *X*-axis, time in hour after the addition of **3a**; *Y*-axis, moles remaining expressed as percent.

they fit the model of a two-step, first-order reaction. The calculated rate constants for the two steps (K_1 and K_2), $t_{1/2}$ values for loss of **3a** and appearance of **1**, and the T_{max} for generation of intermediate **2a** are shown in Table 4. These data confirm the observation that the first step in rat plasma is rapid (K_1 > 10 L/h), while the second conversion proceeds at a more modest rate (K_2 = 0.85 L/h). Conversion rates in pH 8.5 buffer and SIF were significantly slower than those seen in rat plasma but still followed the same pattern. On the basis of these favorable data, compound **3a** was examined in vitro and in vivo for its pharmacological activity and compared to direct administration of **1**.

Table 4. PK Parameters for the Conversion of **3a** to **1** in Rat Plasma, pH 8.5 Buffer, and SIF

medium	K_1 (1/h)	K_2 (1/h)	$t_{1/2}$ of **3a** (h)	t_{max} of **2a** (h)	$t_{1/2}$ of **1** (h)
rat plasma	>10[b]	0.854	<0.07[b]	0.19	0.87
pH 8.5 buffer	0.377	0.0136	1.84	9.14	>24
SIF[a]	0.194	0.0144	3.57	14.48	>24

[a] Simulated intestinal fluid. [b] Could not be accurately determined due to insufficient data points.

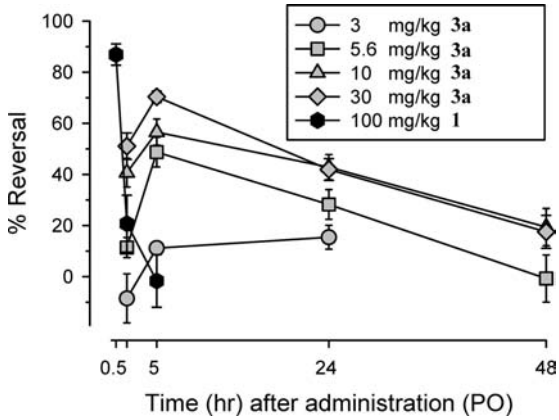

Figure 4. Reversal of PGE_2-induced thermal hypersensitivity after administration of compounds **3a** and **1**: *X*-axis, time in hour after oral compound administration; *Y*-axis, percent reversal of thermal hypersensitivity.

To confirm that the in vivo mechanism of action of **3a** involves conversion to the parent compound **1**, both compounds were evaluated in vitro for their NMDA affinity and functional NMDA antagonist activity. In a rat cortical binding assay, both **3a** and the intermediate hemiester **2a** had low affinity for the competitive NMDA binding site (IC_{50} = 4.2 and 17 μM, respectively) compared to **1** (IC_{50} = 23 nM). Likewise, compound **3a** showed no appreciable inhibition of stimulated TCP binding at high concentrations (8% at 300 μM) compared to **1**, which inhibited this functional measure of NMDA binding with an IC_{50} value of 17 μM. The selectivity of **1** for the competitive glutamate binding site on the NMDA receptor agreed with earlier data[8,11] demonstrating that the compound had little affinity for strychnine-sensitive glycine, kainate, and AMPA receptors (percent inhibition of 33%, 6%, and 17%, respectively, at a concentration of 100 μM).

Compound **3a** reversed PGE_2-induced thermal hypersensitivity in a dose-dependent and time-dependent manner (Figure 4) following oral administration. Importantly, the duration of action of **3a** was substantially longer than that seen with **1**. A low dose of **3a** (3 mg/kg) did not substantially modify thermal hypersensitivity. Higher doses (5.6−30 mg/kg) dose-dependently blocked thermal hypersensitivity with peak effects occurring 5 h after administration and significant effects seen out to at least 24 h. In comparison, an oral dose of 100 mg/kg of **1** produced peak effects at 0.5 h after administration, which declined by 5 h. Potency comparisons evaluated at the time of peak effect (0.5 h for **1**; 5 h for **3a**) indicated that **3a** (ED_{50} = 10 mg/kg) was 3.5-fold more potent than **1** (ED_{50} = 35 mg/kg) in this assay. When converted into molar equivalence (molecular weights: 260 for **1**; 529 for **3a**), this result translated into a 7-fold improvement in potency when **1** was administered as the prodrug **3a**. Moreover, the magnitude of activity shown by **3a** in this model is consistent with the profile of **1** previously described[11] and is not shared by all NMDA antagonists.[1]

Table 5. Average Pharmacokinetic Parameters for the Appearance of **1** Following Equieffective Oral Doses of **1** (30 mg/kg) or **3a** (10 mg/kg) in Male Rats

parameter	**1**	**3a**
dose (mg/kg)	30	10
$t_{1/2}$ (h)	1.3	2.4
T_{max} (h)	0.5	1
C_{max} (ng/mL)	218	254
AUC_{0-4} (ng·h/mL)	342	682
AUC_{0-last} (ng·h/mL)	342	857

On the basis of these data, roughly equieffective doses of **3a** (10 mg/kg, po) and **1** (30 mg/kg, po) were evaluated in pharmacokinetic studies to examine the pharmacokinetic/pharmcodynamic relationship of **3a** and its conversion to **1**. The results are shown in Table 5. Although the 10 mg/kg, po, dose of **3a** yielded the parent compound **1** with a C_{max} value similar to that seen from direct administration of a 30 mg/kg, po, dose of **1**, the time to achieve C_{max} (i.e., T_{max}) and the $t_{1/2}$ were observed later with administration of **3a**, resulting in a larger AUC for **1** when administered as the prodrug. These data suggest that higher exposure levels of **1** are being achieved when given as the prodrug form and are consistent with the 7-fold greater potency seen with **3a** in the behavioral model.

To further characterize the pharmacokinetics of **3a**, biodistribution studies were conducted using 10 mg/kg, po, of [^{14}C]-**3a** and 30 mg/kg, po, of [^{14}C]-**1**. Six time points were examined (0.167, 0.5, 1, 4, 8, and 24 h). Results are presented in Figure 5. Analysis of whole blood, plasma, and brain samples revealed that 88% of the total radioactivity was in the form of compound **1** at the 0.167 time point and that essentially all of the circulating radioactivity (98%) was in the form of compound **1** by 0.5 h. Compound **3a** was not detected at any time point and the hemiester **2a** (10% of total radioactivity) was seen only at the 0.167 h time point. In vitro stability tests confirmed that [^{14}C]-**3a** was not stable in control rat whole blood or plasma, with no [^{14}C]-**3a** detected after 10 min in plasma and after 30 min in whole blood (data not shown). Therefore, measurements of total radioactivity at or after the 0.5 h time point can be attributed to the concentration of compound **1**. Total radioactivity in both plasma and brain were higher after administration of [^{14}C]-**3a**

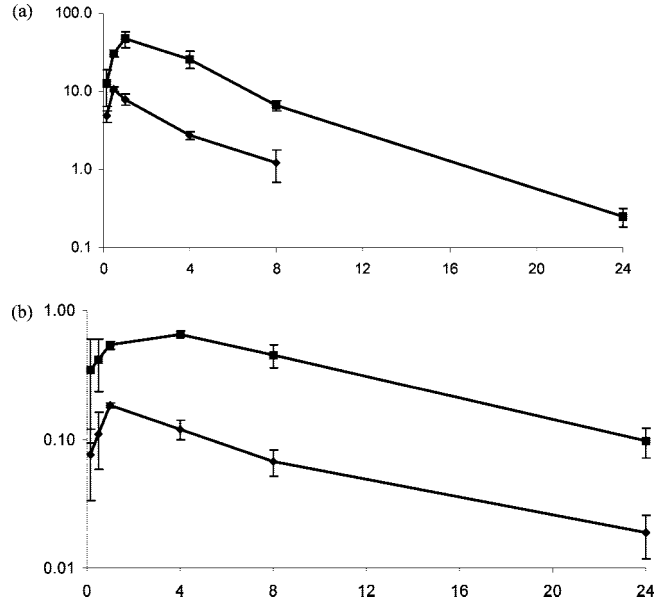

Figure 5. Total radioactivity in plasma (a) and brain (b) after the oral administration of 30 mg/kg [^{14}C]-**1** or 10 mg/kg [^{14}C]-**3a**.

compared to [^{14}C]-**1**. Although plasma and brain elimination $t_{1/2}$ values were approximately equal after administration of [^{14}C]-**3a** and [^{14}C]-**1**, dose-normalized AUC values for total radioactivity in plasma and brain were 7.1-fold and 5.4-fold higher, respectively, following administration of [^{14}C]-**3a** compared to [^{14}C]-**1**. This result was apparently due to a higher C_{max} value seen for [^{14}C]-**3a**. Brain-to-plasma ratios of total radioactivity were similar after administration of either compound.

The pharmacokinetic data are consistent with the pharmacodynamic results seen in the behavioral model. Equieffective doses of **3a** and **1** yielded plasma levels of **1** with similar C_{max} values, and yet **3a** produced a 2-fold higher AUC largely becasue of longer $t_{1/2}$. Together with the lack of substantial affinity for **3a** or the intermediate **2a** at the NMDA receptor, these results suggest that the pharmacodynamic activity of **3a** is related to its conversion to **1**.

Conclusion

In conclusion, we designed and prepared a series of oxymethylene-spaced prodrug candidates of the known competitive NMDA antagonist **1** in an attempt to improve the oral bioavailability of that compound. Initial plasma stability assays identified three molecules (**3a**, **3c**, and **3h**) that released parent compound **1** with the appropriate kinetics to be considered as good potential prodrug candidates. Further physiological stability measurements and consideration of druglike properties (e.g., melting point) led to the selection of compound **3a** for detailed evaluation. Compound **3a** yields **1** via the intermediate hemiester **2a** in vitro in a two-step reaction sequence, with the initial conversion of **3a** to **2a** being considerably more rapid than the decomposition of **2a** to **1**. In a PGE_2-induced thermal hypersensitivity model, orally administered **3a** was more potent at producing antinociceptive effects than **1** (ED_{50} = 10 and 35 mg/kg, respectively). The duration of action of a single, equieffective dose of **3a** was also longer than that seen with **1**. In vitro pharmacological characterization, biodistribution studies, and pharmacokinetic studies indicate that the greater potency and duration of action seen with **3a** correlate with its conversion to **1** and the higher exposure of **1** that is achieved when **3a** is administered. When converted to molar equivalence, these results suggest a 7-fold improvement in potency when **1** is administered in the prodrug form.

Experimental Section

Materials and Methods. Melting points were determined on a Thomas-Hoover capillary or an Electrothermal melting point apparatus and are uncorrected. ^{1}H NMR spectra were recorded on a Varian Unity Plus 400 spectrometer using the residual DMSO signal at 2.49 ppm (ppm) as an internal standard. The chemical shifts are reported in ppm downfield from zero, and coupling constants are reported in hertz (Hz). Solvate, hydrate, and HCl protons are not included. Mass spectra were recorded on a Hewlett-Packard 5995A, a Finnigan Trace MS, or a Micromass LCT spectrometer. C, H, N combustion analyses either were determined on a Perkin-Elmer 2400 analyzer or were performed by Robertson Microlit (Madison, NJ). All analyzed compounds are within ±0.4% of the theoretical value unless otherwise indicated. Flash column chromatography was performed on EM Science silica gel (230−400 mesh). Commercially available reagents and reaction solvents (acetonitrile, dichloromethane, ethyl acetate, hexane) were purchased from Aldrich. The reaction solvents were packaged in Sure/Seal bottles. Solvents for extraction and chromatography (dichloromethane, ethyl acetate) were HPLC-grade OmniSolv reagents purchased from EM Science. The synthesis of compound **1** has been described elsewhere.[8] [^{14}C]-**1** and [^{14}C]-**3a** were provided by Amersham Biosciences[12] and were prepared from [^{14}C]-diethyl squarate using previously described synthetic methodology[8] and the method described below for the synthesis of unlabeled **3a**.

Drugs. Prostaglandin E_2 was purchased from Sigma-Aldrich (St. Louis, MO). For oral dosing, test compounds were suspended in a vehicle consisting of 2% Tween-80 and 0.5% methylcellulose in sterile water. Drug concentration doses (calculated as mg/kg) were calculated using the molecular weight of the base form and were administered in a volume of 1 mL/kg.

Simulated Physiological Fluids. Simulated Gastric Fluid. The fluid was generated by preparing a solution of sodium chloride (0.2 g), concentrated HCl (0.7 mL), and pepsin (Sigma, P-7000, 0.32 g) in deionized water (95 mL). The final volume was adjusted to 100 mL by addition of deionized water.

Simulated Intestinal Fluid. The fluid was generated by preparing a solution of monobasic potassium phosphate (KH_2PO_4, 0.68 g), 0.1 N aqueous sodium hydroxide (38 mL), and pancreatin (Sigma, P-1625, 1 g) in deionized water (57 mL). The pH of the solution was adjusted to 7.5 by addition of 1 N aqueous sodium hydroxide, and then the final volume was adjusted to 100 mL by addition of deionized water.

Simulated Intestinal Bile Fluids. Two stock solutions were first prepared. Stock A consisted of monobasic potassium phosphate (KH_2PO_4, 12.2705 g, 0.0902 M) and sodium chloride (1.7435 g, 0.0298 M) dissolved in 1 L of deionized water. Stock B consisted of dibasic potassium phosphate (K_2HPO_4, 1.7129 g, 0.0098 M) and sodium chloride (1.7435 g, 0.0298 M) dissolved in 1 L of deionized water. SIBLM fed state (pH 5.5) was generated by mixing 72 mL of stock A, 26 mL of stock B, and sodium taurocholate (0.54 g, 10 mM) and then adjusting the final volume to 100 mL with stock B. SIBLM fasted state (pH 6.0) was generated by mixing 44 mL of stock A, 55 mL of stock B, and sodium taurocholate (0.054 g, 1 mM) and then adjusting the final volume to 100 mL with Stock B.

Chemistry. Preparation of 3-{2[8,9-Dioxo-2,6-diazabicyclo[5.2.0-[non-1(7)-en-2-yl}-3-oxido-7-oxo-7-phenyl-2,4,6-trioxa-3-phosphahept-1-yl Benzoate (3a). Chloromethyl Benzoate (4). Zinc chloride (50 mg) was added to paraformaldehyde (4.5 g) at 0 °C. Under stirring and protection from moisture, benzoyl chloride (20 g, 16.5 mL, 142.28 mmol) was slowly added to the reaction mixture over 1 h. The reaction mixture was then heated to 55 °C and stirred at 55 °C for 20 h, cooled to ambient temperature, and left overnight. The reaction mixture was chromatographed on silica gel. Elution with ethyl acetate/hexane (1:1) gave 17 g (∼70%) of the desired ester as a clear oil. ^{1}H NMR (DMSO): δ 7.95−8.0 (d, 2H), 7.68−7.75 (t, 1H), 7.52−7.58 (t, 2H), 6.06 (s, 2H).

3-{2[8,9-Dioxo-2,6-diazabicyclo[5.2.0[non-1(7)-en-2-yl}-3-oxido-7-oxo-7-phenyl-2,4,6-trioxa-3-phosphahept-1-yl Benzoate (3a). Compound **1** (5.25 g, 20.16 mmol) was dissolved in dimethylformamide (120 mL) at ambient temperature. *N*,*N*-Diisopropylethylamine (14 mL, 80.64 mmole) and compound **4** (11.67 g, 68.5 mmol) were added at once, and the reaction mixture was heated to 70 °C for 20 h. After the mixture was cooled to ambient temperature, ethyl acetate (100 mL) was added. The organic solution was washed with saturated aqueous sodium bicarbonate solution followed by brine. The organic layer was dried over anhydrous magnesium sulfate, filtered, and evaporated in vacuo. The residue was subjected to silica gel flash chromatography. Elution with methanol/chloroform/ammonia (7:92:1) gave the desired product, which was crystallized from dichloromethane/ethyl acetate/hexane (6:60:35) to yield 10.5 g (97%) of white microcrystals, mp 124−125 °C. ^{1}H NMR (DMSO): δ 8.46 (s, 1H), 7.95−7.98 (d, 4H), 7.65−7.72 (t, 2H), 7.47−7.52 (t, 4H), 5.81−5.92 (m, 4H), 3.86−3.95 (m, 2H), 3.26−3.34 (t, 2H in the water peak), 3.18−3.23 (t, 2H), 2.36−2.43 (m, 2H), 1.78−1.86 (m, 2H). MS (+ESI) m/z = 528 $(M + H)^+$. Anal. ($C_{25}H_{25}N_2O_9P$) C, H, N.

2,2-Dimethylpropionic Acid (2,2-Dimethylpropioyloxymethoxy)-[2-(8,9-dioxo-2,6-diazabicyclo[5.2.0]non-1(7)-en-2-yl)ethyl)phosphinoyloxymethyl Ester (3b). The title compound was prepared in the same manner as compound **3a** using commercially available chloromethyl 2,2-dimethylpropionate. The desired product was obtained as a viscous oil in 64% yield. ^{1}H NMR (DMSO): δ 8.53 (s, 1H), 5.57−5.65 (m, 4H), 3.87−3.93 (m, 2H), 3.35−3.38 (m,

2H), 3.25−3.28 (m, 2H), 2.28−2.35 (m, 2H), 1.90−1.94 (m, 2H), 1.98 (s, 18H). MS (+ESI) *m/z* 498 $(M + H)^+$. Anal. ($C_{21}H_{33}N_2O_9P$): expected, C (51.64), H (6.81), N (5.73); found, C (50.17), H (6.99), N (5.50).

7-Cyclohexyl-3-{2-[8,9-dioxo-2,6-diazabicyclo[5.2.0]non-1(7)-en-2-yl]ethyl}-3-oxido-7-oxo-2,46-trioxa-3-phosphahept-1-ylcyclohexane Carboxylate (3c). Chloromethyl Cyclohexanecarboxylate (5). This reagent was prepared in the same fashion as compound **4** starting with cyclohexanecarboxylic acid chloride. The product was obtained as a clear oil in 36% yield. ^{1}H NMR (DMSO): δ 5.85 (s, 2H), 1.80−1.87 (m, 2H), 1.64−1.72 (m, 2H), 1.55−1.60 (m, 1H), 1.15−1.42 (m, 6H). MS (+ESI) *m/z* 176 $(M + H)^+$.

7-Cyclohexyl-3-{2-[8,9-dioxo-2,6-diazabicyclo[5.2.0]non-1(7)-en-2-yl]ethyl}-3-oxido-7-oxo-2,46-trioxa-3-phosphahept-1-yl Cyclohexanecarboxylate (3c). The title compound was prepared from **1** in the same fashion as compound **3a** starting with intermediate **4**. The desired product was obtained after crystallization from ethyl acetate/diethyl ether/hexane (6:1:3) as a white solid in 53% yield, mp 64−65 °C. ^{1}H NMR (DMSO): δ 8.54 (s, 1H), 5.7−6.2 (m, 4H), 3.85−3.93 (m, 2H), 3.35−3.4 (m, 2H), 3.25−3.27, (t, 2H), 2.38−2.41 (m, 2H), 2.28−2.33 (m, 2H), 1.83−1.98 (m, 4H), 1.65−1.72 (d, 4H), 1.58−1.62 (d, 2H), 1.17−1.40 (m, 10H). MS (+ESI) *m/z* 541 $(M + H)^+$. Anal. ($C_{25}H_{37}N_2O_9P$) C, H, N.

3-{2-[8,9-Dioxo-2,6-diazabicyclo[5.2.0]non-1(7)-en-2-yl]ethyl}-1,5-dimethyl-3-oxido-7-oxo-7-phenyl-2,4,6-trioxa-3-phosphahept-1-yl Benzoates 3d (Diastereomer 1) and 3e (Diastereomer 2). 1-Chloroethyl Benzoate (7). Zinc chloride (0.2 g) was added to benzoyl chloride (20 g, 20.63 mL, 177.85 mmol) at −20 °C. Under stirring and protection from moisture, acetaldehyde (10 mL, 178.88 mmol) was added dropwise. After the addition, the reaction mixture was stirred at −20 °C for 1 h. Thereafter, the reaction mixture was allowed to reach ambient temperature and stirring was continued for 20 h. The reaction mixture was concentrated in vacuo and flash-chromatographed on silica gel. Elution with ethyl acetate/hexane (1:9) gave 22.4 g (68%) of the desired ester as a clear oil. ^{1}H NMR (DMSO): δ 8.00−8.05 (d, 2H), 7.72−7.77 (t, 1H), 7.57−7.61 (t, 2H), 6.8−6.85 (q, 1H), 1.9−1.93 (d, 3H). MS (+ESI) *m/z* = 184 $(M + H)^+$.

3-{2-[8,9-Dioxo-2,6-diazabicyclo[5.2.0]non-1(7)-en-2-yl]ethyl}-1,5-dimethyl-3-oxido-7-oxo-7-phenyl-2,4,6-trioxa-3-phosphahept-1-yl Benzoates 3d (Diastereomer 1) and 3e (Diastereomer 2). The diastereomeric mixture of compounds **3d** and **3e** was prepared from compound **1** in the same fashion as compound **3a** using intermediate **7**. After the reaction workup the diastereomers were separated by flash column chromatography on silica gel.

Elution with 8% methanol/chloroform gave 7% of the first diastereomer compound **3d** as a yellow glasslike material. ^{1}H NMR (DMSO): δ 8.41 (s, 1H), 7.92−7.96 (d, 4H), 7.63−67 (t, 2H), 7.44−7.53 (t, 4H), 6.21−6.26 (2H), 3.8−3.87 (m, 2H), 3.22.3.30 (m, 2H), 3.15−3.19 (m, 2H), 2.24−2.34 (m, 2H), 1.77−1.81 (m, 2H), 1.53−1.58 (d, 6H). MS (+ESI) *m/z* = 557 $(M + H)^+$. Anal. ($C_{27}H_{29}N_2O_9P$) C, H, N.

Further elution with 8% methanol/chloroform afforded compound **3e** as a yellow glasslike material in 16% yield. ^{1}H NMR (DMSO): δ 8.42 (s, 1H), 7.9−7.96 (m, 4H), 7.62−7.68 (q, 2H), 7.45−7.54 (m, 4H), 6.7−6.75 (m, 1H), 6.61−6.67 (m, 1H), 3.93−4.02 (m, 1H), 3.73−3.84 (m, 1H), 3.24−3.30 (m, 2H), 3.15−3.20 (m, 2H), 2.23−2.36 (m, 2H), 1.77−1.82 (t, 2H), 1.56−1.59 (d, 3H), 1.43−1.46 (s, 3H). MS (+ESI) *m/z* = 557 $(M + H)^+$. Anal. ($C_{27}H_{29}N_2O_9P$) C, H, N.

7-Cyclohexyl-3-{2-[8,9-dioxo-2,6-diaza[5.2.0]non-1(7)-en-2-yl]ethyl}-1,5-dimethyl-3-oxido-7-oxo-2,4,6-trioxa-3-phosphahept-1-yl Cyclohexanecarboxylate (3f). 1-Chloroethyl Cyclohexanecarboxylate (8). This reagent was prepared in the same manner as intermediate **7** starting with cyclohexanecarboxylic acid chloride. The product was obtained as a clear oil in 53% yield and was used without further purification. MS (+ESI) *m/z* = 191 $(M + H)^+$.

7-Cyclohexyl-3-{2-[8,9-dioxo-2,6-diaza[5.2.0]non-1(7)-en-2-yl]ethyl}-1,5-dimethyl-3-oxido-7-oxo-2,4,6-trioxa-3-phophsphahept-1-yl Cyclohexanecarboxylate (3f). The title compound was prepared from **1** in the same fashion as compound **3a** using intermediate **8**. After workup, the crude reaction mixture was purified by flash chromatography on silica gel. Elution with 3% methanol/ethyl acetate gave the desired product as a yellow oil in 16% yield. ^{1}H NMR (DMSO): δ 8.51 (s, 1H), 6.43−6.46 (m, 1H), 6.38−6.42 (m, 1H), 3.90−3.97 (m, 1H), 3.75−3.82 (m, 1H), 3.34−3.38 (m, 2H), 3.23−3.26 (m, 2H), 2.30−2.37 (m, 2H), 2.20−2.28 (m, 2H), 1.87−1.92 (t, 2H), 1.78−1.83 (m, 4H), 1.62−1.67 (m, 4H), 1.54−1.59 (m, 2H), 1.42−1.45 (2d, 6H), 1.12−1.27 (m, 10H). MS (ESI−) *m/z* = 567 $(M - H)^-$. Anal. ($C_{27}H_{41}N_2O_9P$) C, H, N.

3-{2-[8,9-Dioxo-2,6-diazabicyclo[5.2.0]non-1(7)-en-2-yl]ethyl}-3-oxido-7-oxo-8-propyl-2,4,6-trioxa-3-phosphaundec-1-yl 2-Propylpentanoate (3g). Chloromethyl 2-Propylpentanoate (6). The reagent was prepared in the same manner as intermediate **4** starting with 2-propylbutanoic acid. The product was obtained as an oil in 75% yield and was used without further purification. MS (+ESI) *m/z* = 193 $(M + H)^+$.

3-{2-[8,9-Dioxo-2,6-diazabicyclo[5.2.0]non-1(7)-en-2-yl]ethyl}-3-oxido-7-oxo-8-propyl-2,4,6-trioxa-3-phosphaundec-1-yl 2-Propylpentanoate (3g). This compound was prepared from **1** in the same fashion as compound **3a** using intermediate **6**. After workup, the crude reaction mixture was purified by flash chromatography on silica gel. Elution with 8% methanol/ethyl acetate gave the desired product in 56% yield as a colorless oil which solidified upon standing. ^{1}H NMR (DMSO): δ 8.57 (s, 1H), 5.58−5.66 (m, 4H), 3.94−3.93 (m, 2H), 3.34−3.37 (m, 2H), 3.26−3.29 (m, 2H), 2.39−2.43 (m, 2H), 2.25−2.35 (m, 2H), 1.89−1.95 (m, 2H), 1.52−1.58 (m 4H), 1.4−1.45 (4H), 1.21−1.30 (m, 8H) 0.82−0.87 (t, 12H). MS (+ESI) *m/z* = 573 $(M + H)^+$. Anal. ($C_{27}H_{45}N_2O_9P$) C, H, N.

7-Bis{[(isopropoxycarbonyl)oxy]methyl}-{2-[8,9dioxo-2,6-diazabicyclo[5.2.0]non-1(7)-en-2-yl]ethyl}phosphonate (3h). Chloromethyl Isopropylcarbonate (9). A solution of chloromethyl chloroformate (6.5 mL, 73.85 mmol) and 2-propanol (5.6 mL, 73.14 mmole) in diethyl ether (100 mL) was cooled to 0 °C. Pyridine (6 mL, 74.18 mmol) was added dropwise. Thereafter, the ice bath was removed and the reaction mixture was allowed to reach ambient temperature and was stirred for 20 h. The formed solids were filtered and washed with ethyl ether. The the combined supernatant was washed with aqueous 1% citric acid followed by aqueous 1% $NaHCO_3$ and brine. After evaporation of the solvent in vacuo, the desired product was obtained as a clear oil (10.26 g, 92%). ^{1}H NMR (DMSO): δ 5.82 (s, 2H); 4.77−4.86 (m, 1H), 1.2−1.23 (d, 6H). MS (ESI+) *m/z* = 152 $(M + H)^+$.

7-Bis{[(isopropoxycarbonyl)oxy]methyl}-{2-[8,9dioxo-2,6-diazabicyclo[5.2.0]non-1(7)-en-2-yl]ethyl}phosphonate (3h). The title compound was prepared from **1** in the same fashion as compound **3a** using intermediate **9**. After workup the crude reaction mixture was crystallized from ethyl acetate/diethyl ether/hexane (6:1:3) to yield the desired product as an off-white solid in 44% yield. ^{1}H NMR (DMSO): δ 8.46 (s, 1H), 4.75−4.83 (m, 2H), 3.80−3.87 (m, 2H), 3.32−3.35 (m, 2H), 3.20−3.24 (m, 2H), 2.23−2.35 (m, 2H), 1.82−1.88 (m, 2H), 1.18−1.22 (d, 12H). MS (ESI+) *m/z* = 493 $(M + H)^+$. Anal. ($C_{19}H_{29}N_2O_{11}P$) C, H, N.

Pharmacology Methods. Animals. Animal maintenance and research were conducted in accordance with the National Research Council's policies and guidelines for the handling and use of laboratory animals outlined in the Guide for the Care and Use of Laboratory Animals (National Research Council, 1996). The laboratory facility was licensed by the United States Department of Agriculture and accredited by the American Association for Accreditation of Laboratory Animal Care. Research protocols were approved by the Wyeth Institutional Animal Care and Use Committee in accordance with the guidelines of the Committee for Research and Ethical Issues of the International Association for the Study of Pain.[13]

Binding Assays. Membranes derived from rat whole brain were prepared as previously described for [^{3}H]-CGP-39653 (NMDA recognition site), [^{3}H]-TCP (PCP site), and [^{3}H]-glycine binding assays,[14] whereas rat frontal cortex and forebrain membranes were used as previously reported for [^{3}H]-kainate and [^{3}H]-AMPA binding assays, respectively.[15] Competition binding experiments

utilizing [^{3}H]-CGP-39653, [^{3}H]-glycine, [^{3}H]-kainic acid, and [^{3}H]-AMPA were carried out as previously described.[16−19] Functional [^{3}H]-TCP binding assays were performed as previously described[19] with modifications.[10] Competition binding curves were fitted with a four-parameter logistic model, which defined IC_{50} values for compounds **1** and **3a** (GraphPad Prism, San Diego, CA).

PGE_2-Induced Thermal Hypersensitivity. Male Charles River Sprague−Dawley rats (Kingston/Stoneridge, NY) weighing 200−250 g at time of arrival were individually housed in wire cages in a climate-controlled room. A 12 h light/dark cycle (lights on at 06:30) was in effect for all animals, and water was available ad libitum. For all oral dosing studies, rats were fasted for approximately 16 h before drug administration. To assess baseline thermal sensitivity, the terminal 10 cm of the tail was placed into water warmed to 34, 38, 42, 46, 50, 54, or 58 °C. The latency in seconds for the animal to remove the tail from the water was used as a measure of nociception. If the animal did not remove the tail within 20 s, the experimenter removed the tail and a maximum latency of 20 s was recorded. Following the assessment of baseline thermal sensitivity, thermal hypersensitivity was produced by an intradermal 50 μL injection of 0.1 mg of PGE_2 (Sigma, St. Louis, MO). Temperature−effect curves were generated before (baseline) and after (30 min) PGE_2. On the basis of previous results,[20] subjects were tested a maximum of three times with a minimum of 5 days between tests (one baseline 0.1 mg PGE_2 assessment and one or two compound tests in the presence of 0.1 mg of PGE_2). The ability of compounds to block 0.1 mg PGE_2-induced thermal hypersensitivity was assessed using a single dose procedure. Under this procedure, a single dose of compound was administered ip or po at 0.5, 1.7, 3, 5, 24, or 48 h before the injection of PGE_2 and thermal sensitivities were assessed 30 min after PGE_2 injection.

Temperature−effect curves were generated for each experimental condition for individual rats. The temperature that produced a half-maximal increase in the tail-withdrawal latency (i.e., T_{10}) was calculated from each temperature−effect curve. The T_{10} was determined by interpolation from a line drawn between the point above and the point below 10 s on the temperature−effect curve. For these studies, thermal hypersensitivity was defined as a leftward shift in the temperature−effect curve and a decrease in the T_{10} value. Reversal of thermal hypersensitivity was defined as a return to baseline of the temperature−effect curve and the T_{10} value. Blockade of irritant-induced thermal hypersensitivity was quantified as the percentage return to baseline values (% reversal) according to the following equation:

$$\%\ \text{reversal} = \frac{(T_{10}^{\text{drug+irritant}}) - (T_{10}^{\text{irritant}})}{(T_{10}^{\text{baseline}}) - (T_{10}^{\text{irritant}})} \times 100$$

in which $T_{10}^{\text{drug+irritant}}$ is the T_{10} after a drug in combination with PGE_2 or capsaicin, T_{10}^{irritant} is the T_{10} after PGE_2 or capsaicin alone, and T_{10}^{baseline} is the T_{10} under control conditions. Statistical analysis was done using a within-subjects-repeated-measures analysis of variance on T_{10} values. The criterion for significant reversal of the T_{10} value from the chemical irritant alone was $p < 0.05$.

In Vitro Stability Studies. Physiological Stability. The physiological stability of derivative **3a** was determined by examining the stability of the compound in a series of buffers with pH values ranging from 1 to 9 as well as in SGF, SIF, and SIBLM at 37 °C. The compounds were prepared in a 9:1 mixture of the appropriate test component (buffer, SGF, SIF, or SIBLM) and acetonitrile to a final concentration of 0.01 mg/mL according to the procedure described in the Supporting Information. The samples were thoroughly mixed and placed in an autosampler maintained at 37 °C. Each sample was injected consecutively onto the system (Inertsil C8-3, 3 μm, 150 mm × 4.6 mm; 1 mL/min; mobile phase of 0.1% formic acid in water/0.1% formic acid in acetonitrile; MS scan range of 200−1000 *m*/*z*, 60 psi, 12.0 L/min, 350 °C) every 4 h over a 24 h period. The percent remaining at each injection time was calculated on the basis of the area comparison of compound peak at 304 nm, corrected by an internal standard. The identities of the parent compounds and conversion products were confirmed by LC/MS (−ESI, scan range 200−1000 *m*/*z*, 60 psi, 12.0 L/min, 350 °C). The kinetics of the conversion reactions were analyzed by MicroMath Scientist software.

Plasma Stability. The in vitro physiological stability of compounds **3a**−**h** in rat plasma was determined by dissolving the compounds in rat plasma to a concentration of 0.05 mg/mL. Aliquots of 0.5 mL of the compound/plasma mixture were placed separately into extraction tubes and incubated at 37 °C for 0, 0.25, 0.5, 1, 3, 5, 7, and 24 h, respectively. At the appropriate time, the plasma sample was treated with 0.5 mL of acetonitrile and centrifuged. The supernatant was diluted with deionized water and injected onto the HPLC system (Inertsil C8-3, 3 μm, 150 mm × 4.6 mm; 1 mL/min; mobile phase of 0.1% formic acid in water/0.1% formic acid in acetonitrile). The percentage of the parent compound and conversion products in plasma were calculated on the basis of area comparison of their peaks at 304 nm, corrected by an internal standard. The identities of the parent compounds and conversion products were confirmed by LC/MS (−ESI, scan range 200−1000 *m*/*z*, 60 psi, 12.0 L/min, 350 °C). The kinetics of the conversion reactions were analyzed by MicroMath Scientist software.

Pharmacokinetic Studies. Male Sprague−Dawley rats were administered either **1** (30 mg/kg po) or **3a** (10 mg/kg po) via oral gavage. These doses were chosen because they are pharmacologically equivalent. Plasma samples were taken at 0, 0.25, 0.5, 1, 2, 4, and 6 h following administration. The number of animals per time point were $n = 2$ for 0, 2, 4, and 6 h and $n = 3$ for 0.25, 0.5, and 1 h. Plasma samples were stabilized by adding 5 μL of glacial acetic acid and 10 μL of 300 mM aqueous potassium fluoride solution. For MS, the plasma samples were acidified using 20 mL of 1 N HCl and extracted into 4 volumes of *n*-butanol. The butanol layer was concentrated to dryness in vacuo and reconstituted into 100 μL of water for injection onto the HPLC system (Aquasil C18, 3 μm, 2 mm × 20 mm; temperature of 50 °C; autosampler temperature of 10 °C; 1 mL/min; 4:1 split into mass spectrometer, 200 μL/min into the mass spectrometer; mobile phase of 0.1% formic acid in water/0.1% formic acid in acetonitrile). Pharmacokinetic parameters were calculated using IBIS (version 1.5.0), DMAS (version 1.2), or WinNonlin (version 2.1) software.

Radiolabeled Oral Bioavailability Studies. Male Sprague−Dawley rats were administered either [^{14}C]-**1** (30 mg/kg) or [^{14}C]-**3a** (10 mg/kg) via oral gavage. Blood, plasma, and brain ($n = 3$ rats/time point) were collected at 0.167, 0.5, 1, 4, 8, and 24 h postdose. Radioactivity concentrations were determined in each matrix. Metabolite profiles in plasma and brain were determined using HPLC (Aquasil C18, 3 μm, 2 mm × 20 mm; temperature of 50 °C; autosampler temperature of 10 °C; 1 mL/min; mobile phase of 0.1% formic acid in water/0.1% formic acid in acetonitrile) with in-line radioactivity detection. The stability of [^{14}C]-**3a** in control rat whole blood and plasma incubated at 37 °C was also determined.

Acknowledgment. The authors thank Wyeth Discovery Analytical Chemistry for their assistance in the structural confirmation of the compounds described in this manuscript and for their help with HPLC separations. The authors also thank Amersham Biosciences for supplying [^{14}C]-**1** and [^{14}C]-**3a**.

Supporting Information Available: Results from elemental analysis for compounds **3a**−**h** and experimental protocol for the preparation of samples for physiological stability measurements. This material is available free of charge via the Internet at http://pubs.acs.org.

References

(1) Sluka, K. A.; Westlund, K. N. Spinal cord amino acid release and content in an arthritis model: the effects of pretreatment with non-NMDA, NMDA, and NK1 receptor antagonists. *Brain Res.* **1993**, *627*, 89–103.

(2) Kawamata, M.; Omote, K. Involvement of increased excitatory amino acids and intracellular Ca^{2+} concentration in the spinal dorsal

horn in an animal model of neuropathic pain. *Pain* **1996**, *68*, 85–96.

(3) Dickenson, A. H.; Chapman, V.; Green, G. M. The pharmacology of excitatory and inhibitory amino acid-mediated events in the transmission and modulation of pain in the spinal cord. *Gen. Pharmacol.* **1997**, *28*, 633–638.

(4) Mao, J.; Price, D. D.; Hayes, R. L.; Lu, J.; Mayer, D. J.; et al. Intrathecal treatment with dextrorphan or ketamine potently reduces pain-related behaviors in a rat model of peripheral mononeuropathy. *Brain Res.* **1993**, *605*, 164–168.

(5) Chaplan, S. R.; Malmberg, A. B.; Yaksh, T. L. Efficacy of spinal nmda receptor antagonism in formalin hyperalgesia and nerve injury evoked allodynia in the rat. *J. Pharmacol. Exp. Ther.* **1997**, *280*, 829–838.

(6) Suzuki, R.; Matthews, E. A.; Dickenson, A. H. Comparison of the effects of MK-801, ketamine and memantine on responses of spinal dorsal horn neurones in a rat model of mononeuropathy. *Pain* **2001**, *91*, 101–109.

(7) Kristensen, J. D.; Svensson, B.; Gordh, T., Jr. The NMDA-receptor antagonist CPP abolishes neurogenic "wind-up pain" after intrathecal administration in humans. *Pain* **1992**, *51*, 249–253.

(8) Kinney, W. A.; Abou-Gharbia, M.; Garrison, D. T.; Schmid, J.; Kowal, D. M.; et al. Design and synthesis of [2-(8,9-dioxo-2,6-diazabicyclo-[5.2.0]non-1(7)-en-2-yl)-ethyl]phosphonic acid (EAA-090), a potent *N*-methyl-D-aspartate antagonist, via the use of 3-cyclobutene-1,2-dione as an achiral alpha-amino acid bioisostere. *J. Med. Chem.* **1998**, *41*, 236–246.

(9) Childers, W. E.; Abou-Gharbia, M. A.; Moyer, J. A.; Zaleska, M. M. EAA-090, neuroprotectant, competitive NMDA antagonist. *Drugs Future* **2002**, *27*, 633–638.

(10) Sun, L.; Chiu, D.; Kowal, D.; Simon, R.; Smeyne, M.; et al. Characterization of two novel *N*-methyl-D-aspartate antagonists: EAA-090 (2-[8,9-dioxo-2,6-diazabicyclo [5.2.0]non-1(7)-en2-yl-]ethylphosphonic acid) and EAB-318 (*R*-alpha-amino-5-chloro-1-(phosphonomethyl)-1*H*-benzimidazole-2-propanoic acid hydrochloride). *J. Pharmacol. Exp. Ther.* **2004**, *310*, 563–570.

(11) Brandt, M. R.; Cummons, T. A.; Potestio, L.; Sukoff, S. J.; Rosenzweig-Lipson, S. Effects of the *N*-methyl-D-aspartate receptor antagonist perzinfotel [EAA-090; [2-(8,9-dioxo-2,6-diazabicyclo[5.2.0 non-1(7)-en-2-yl)-ethyl]phosphonic acid] on chemically-induced thermal hypersensitivity. *J. Pharmacol. Exp. Ther.* **2005**, *313*, 1379–1386.

(12) Amersham Biosciences, part of GE Healthcare Life Sciences, 800 Centennial Avenue, P.O. Box 1327, Piscataway, NJ 08855.

(13) Zimmermann, M. Ethical guidelines for investigations of experimental pain in conscious animals. *Pain* **1983**, *16*, 109–110.

(14) Murphy, D. E.; Schneider, J.; Boehm, C.; Lehmann, J.; Williams, J. Binding of [^{3}H]3-(2-carboxypiperazin-4-yl)propyl-1-phosphonic acid to rat membranes: a selective, high-affinity ligand for *N*-methyl-D-aspartate receptors. *J. Pharmacol. Exp. Ther.* **1987**, *240*, 778–783.

(15) London, E. D.; Coyle, J. T. Specific binding of [^{3}H]kainic acid receptor sites in rat brain. *Mol. Pharmacol.* **1979**, *15*, 492–505.

(16) Sills, M. A.; Fagg, G.; Pozza, M.; Angst, C.; Brundish, D. E.; Hurt, S. D.; Wilusz, E. J.; Williams, M. [^{3}H]CGP 39653; a new *N*-methyl-D-aspartate antagonist radioligand with low nanomolar affinity in rat brain. *Eur. J. Pharmacol.* **1991**, *192*, 19–24.

(17) Monahan, J. B.; Corpus, V. M.; Hood, W. F.; Thomas, J. W.; Compton, R. P. Characterization of a [^{3}H]glycine recognition site as a modulatory site of the *N*-methyl-D-aspartate receptor complex. *J. Neurochem.* **1989**, *53*, 370–375.

(18) Murphy, D. E.; Showhill, E. W.; Williams, M. Characterization of quisqualate recognition sites in rat train tissue using DL-[^{3}H]-α-amino-3-hydroxy-5-methylisoxazole-4-propionic acid (AMPA) and a filtration assay. *Neurochem. Res.* **1987**, *12*, 775–782.

(19) Ransom, R. W.; Stec, N. L. Cooperative modulation of [^{3}H]MK-801 binding to the *N*-methyl-D-aspartate receptor-ion channel complex by L-glutamate, glycine, and polyamines. *J. Neurochem.* **1988**, *51*, 830–836.

(20) Brandt, M. R.; Furness, M. S.; Mello, N. K.; Rice, K. C.; Negus, S. S. Antinociceptive effects of delta-opioid agonists in rhesus monkeys: effects on chemically-induced thermal hypersensitivity. *J. Pharamcol. Exp. Ther.* **2001**, *296*, 939–946.

JM8011799